

Critical current of spin-transfer-torque-driven magnetization dynamics in magnetic multilayers

Tomohiro Taniguchi^{1,2} and Hiroshi Imamura^{1,*}¹*Nanotechnology Research Institute, AIST, Tsukuba, Ibaraki 305-8568, Japan*²*Institute of Applied Physics, University of Tsukuba, Tsukuba, Ibaraki 305-8573, Japan*

(Received 11 June 2008; revised manuscript received 29 September 2008; published 31 December 2008)

The critical current of the spin-transfer-torque-driven magnetization dynamics was studied by taking into account both spin pumping and the finite penetration depth of the transverse spin current. We successfully reproduced the recent experimental results obtained by Chen *et al.* [Phys. Rev. B **74**, 144408 (2006)] and found that the critical current remains finite even in the zero-thickness limit of the free layer. We showed that the remaining value of the critical current is determined mainly by spin pumping. We also showed that we could control the critical current by varying the spin-diffusion length of the nonmagnetic electrode adjacent to the free layer.

DOI: [10.1103/PhysRevB.78.224421](https://doi.org/10.1103/PhysRevB.78.224421)

PACS number(s): 75.70.Cn, 72.25.Ba, 73.23.-b, 76.60.Es

Spin transfer torque (STT) is the torque due to the transfer of transverse spin angular momentum from the conducting electrons to the magnetization of a ferromagnet.^{1,2} The STT in magnetic multilayers such as the current perpendicular-to-the-plane giant magnetoresistive (CPP-GMR) (Refs. 3–5) and tunnel magnetoresistive (TMR) (Refs. 6–8) spin valves has been investigated intensively because STT-driven magnetization dynamics is a promising technique in operating the spin-electronic devices such as magnetic random access memories and microwave oscillators. One of the main obstacles in developing STT-based spin-electronic devices is the high critical current density. The critical current density required to induce the STT-driven magnetization dynamics in CPP-GMR spin valves is as high as 10^6 – 10^8 A/cm².^{9–12}

On the other hand, the CPP-GMR spin valve is one of the promising candidates for the read head for ultrahigh-density magnetic recording.^{13,14} It is known that STT-driven magnetization dynamics produces noise, and that low critical current density is required for the read head application.¹⁵ Therefore, it is natural to ask how to control the critical current density of STT-driven magnetization dynamics in CPP-GMR spin valves.

STT was first proposed by Slonczewski¹ and independently by Berger² in 1996. In Slonczewski's theory the critical current of STT-driven magnetization dynamics is expressed as^{16,17}

$$I_c = \frac{2eMSd}{\hbar\gamma\eta} \alpha_0 \omega, \quad (1)$$

where e is the elementary charge and \hbar is the Dirac constant. M , S , d , γ , and α_0 are the magnetization, cross-section area, thickness, gyromagnetic ratio, and intrinsic Gilbert damping constant of the free layer, respectively. ω is the angular frequency of the magnetization around the equilibrium point. The transverse spin-polarization coefficient η depends only on the relative angle of the magnetizations of the fixed and free layers.^{1,16} According to Slonczewski's theory, we can control the critical current by varying the thickness of the free layer d and the critical current vanishes in the limit of $d \rightarrow 0$.

However, recently, Chen *et al.*¹² reported that the critical current of STT-driven magnetization dynamics of a CPP-GMR spin valve remains finite even in the zero-thickness limit of the free layer. What are missing from the above consideration based on Slonczewski's theory are the effects of the finite penetration depth of the transverse spin current, λ_t ,^{18–20} and spin pumping.^{20–24} The penetration depth of the transverse spin current is the characteristic length of the ferromagnetic (F) metal over which the transfer of the spin angular momentum from conducting electrons to the magnetization is achieved. If the free layer is thinner than λ_t , the conducting electrons cannot transfer their angular momentum to the magnetization to exert STT. Spin pumping is the phenomenon by which the spin current is pumped out from the free layer into the other layers. The magnetic (Gilbert) damping of the free layer is enhanced by spin pumping. Therefore, we need to analyze the experimental results by taking into account both the finite penetration depth of the transverse spin current and spin pumping to understand the mechanism that determines the critical current of STT-driven magnetization dynamics in magnetic multilayers.

In this paper, we study the critical current of STT-driven magnetization dynamics by taking into account both the finite penetration depth of the transverse spin current and spin pumping. In order to analyze the experiments by Chen *et al.*,¹² we extend the spin-pumping theory with the finite penetration depth²⁰ to include the electric current. We show that the critical current remains finite even in the zero-thickness limit of the free layer, which agrees quantitatively well with the results of Ref. 12, and that the remaining value is determined mainly by spin pumping. We found that we can control the remaining value of the critical current by varying the spin-diffusion length of the nonmagnetic (N) electrode adjacent to the free layer. The longer the spin-diffusion length of the nonmagnetic electrode, the smaller the remaining value of the critical current.

The system we consider is shown in Fig. 1. Two ferromagnetic layers (F_1 and F_2) are sandwiched by the nonmagnetic layers N_i ($i=1-7$). The F_1 and F_2 layers correspond to the free and fixed layers, respectively. \mathbf{m}_k ($k=1,2$) is the unit vector pointing to the direction of the magnetization of the F_k layer. d_k and L_i are the thicknesses of the F_k and N_i layers,

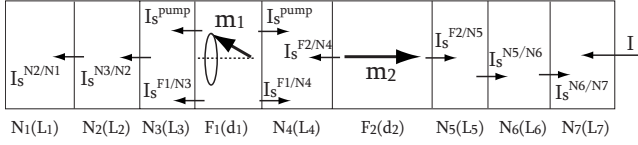


FIG. 1. The nonmagnetic (N)/ferromagnetic (F) multilayer, i.e., CPP-GMR spin valve, we consider is schematically shown. The symbols are defined in the text.

respectively. The electric current I flows from the N_7 layer to the N_1 layer.

In order to analyze the STT-driven magnetization dynamics in the multilayer system shown in Fig. 1, we extend the spin-pumping theory with the finite penetration depth²⁰ to include the electric current. The electric and pumped spin currents at the F_k/N_i interface (into N_i) are derived by the circuit theory,²⁵ and expressed in terms of the charge accumulation μ_{N_i, F_k} and the spin accumulation μ_{N_i, F_k}^s as^{23,25}

$$I^{F_k/N_i} = \frac{eg}{2h} \{2(\mu_{F_k} - \mu_{N_i}) + p\mathbf{m}_k \cdot (\mu_{F_k} - \mu_{N_i})\}, \quad (2)$$

$$\mathbf{I}_s^{\text{pump}} = \frac{\hbar}{4\pi} \left(g_r^{\uparrow\downarrow} \mathbf{m}_1 \times \frac{d\mathbf{m}_1}{dt} + g_i^{\uparrow\downarrow} \frac{d\mathbf{m}_1}{dt} \right), \quad (3)$$

where $h=2\pi\hbar$ is the Planck constant, $g=g^{\uparrow\uparrow}+g^{\downarrow\downarrow}$ is the sum of the spin-up and spin-down conductances, $p=(g^{\uparrow\uparrow}-g^{\downarrow\downarrow})/(g^{\uparrow\uparrow}+g^{\downarrow\downarrow})$ is the spin polarization of the conductances, and $g_{r(i)}$ is the real (imaginary) part of the mixing conductance. The spin current at each F_k/N_i and N_i/N_j interfaces (into N_i) are given by^{20,25}

$$\begin{aligned} \mathbf{I}_s^{F_k/N_i} = & \frac{1}{4\pi} \left[g \left\{ p(\mu_{F_k} - \mu_{N_i}) + \frac{1}{2} \mathbf{m}_k \cdot (\mu_{F_k} - \mu_{N_i}) \right\} \mathbf{m}_k \right. \\ & - g_r^{\uparrow\downarrow} \mathbf{m}_k \times (\mu_{N_i} \times \mathbf{m}_k) - g_i^{\uparrow\downarrow} \mu_{N_i} \times \mathbf{m}_k \\ & \left. + t_r^{\uparrow\downarrow} \mathbf{m}_k \times (\mu_{F_k} \times \mathbf{m}_k) + t_i^{\uparrow\downarrow} \mu_{F_k} \times \mathbf{m}_k \right], \quad (4) \end{aligned}$$

$$\mathbf{I}_s^{N_i/N_j} = -\frac{g_{N_i/N_j}}{4\pi} (\mu_{N_i} - \mu_{N_j}), \quad (5)$$

where $t_{r(i)}^{\uparrow\downarrow}$ is the real (imaginary) part of the transmission mixing conductance at the F_k/N_i interface and g_{N_i/N_j} is the conductance of the one spin channel at the interface. The spin current of Eq. (4) is obtained from the circuit theory of Brataas *et al.*,²⁵ eliminating the assumption that the nonequilibrium distribution function of the electrons in a ferromagnetic layer is aligned to the direction of the magnetization in spin space. It should be noted that the transmission mixing conductance in Eq. (4) is different from that defined by Zwierzycki *et al.*²⁶ Zwierzycki *et al.*²⁶ calculated a transmission mixing conductance defined through a $N/F/N$ junction defined as $t^{\uparrow\downarrow} = t^{\uparrow} t^{\downarrow*}$, where $t^\sigma = t_{F \rightarrow N}^\sigma e^{ik_\perp^\sigma d} t_{N \rightarrow F}^\sigma$ and $t_{F(N) \rightarrow N(F)}^\sigma$ is the transmission coefficient for electrons from $F(N)$ to $N(F)$, and showed that $t^{\uparrow\downarrow}$ depends on the thickness of the ferromagnetic layer d due to the phase factor $e^{ik_\perp^\sigma d}$.²⁶ On the other hand, the transmission mixing conductance in Eq. (4) is de-

finied by $t_{r(i)}^{\uparrow\downarrow} = \text{Re}(\text{Im})[t_{F \rightarrow N}^\uparrow t_{F \rightarrow N}^{\downarrow*}]$, and is independent of the thickness of the ferromagnetic layer. Although the original formulation of the circuit theory assumed the spatially uniform charge and spin accumulations,²⁵ it has been shown that the circuit theory is applicable to the diffusive system.^{24,27} It should be noted that there is a controversial issue regarding the transverse spin accumulation in the ferromagnetic layer, $\mu_F^T = \mathbf{m} \times (\mu_F \times \mathbf{m})$.^{18,19,23–25,28–30}

The spin accumulation in the nonmagnetic layer μ_N obeys the diffusion equation,³¹ and is expressed as a linear combination of $\exp(\pm x/\lambda_{\text{sd}(N)})$, where $\lambda_{\text{sd}(N)}$ is the spin-diffusion length of the nonmagnetic layer. The spin current in the nonmagnetic layer is given by

$$\mathbf{I}_s^N = -\frac{\partial}{\partial x} \frac{\hbar S \sigma_N}{2e^2} \mu_N, \quad (6)$$

where σ_N is the conductivity of the nonmagnetic layer.

The longitudinal spin accumulation in the ferromagnetic layer, $\mu_F^L = (\mathbf{m} \cdot \mu_F) \mathbf{m}$, also satisfies the diffusion equation and is expressed as a linear combination of $\exp(\pm x/\lambda_{\text{sd}(F_L)})$, where $\lambda_{\text{sd}(F_L)}$ is the longitudinal spin-diffusion length of the ferromagnetic layer.³¹ The longitudinal spin current in the ferromagnetic layer is

$$(\mathbf{m} \cdot \mathbf{I}_s^F) \mathbf{m} = -\frac{\partial}{\partial x} \frac{\hbar S}{2e^2} (\sigma_F^\uparrow \mu_F^\uparrow - \sigma_F^\downarrow \mu_F^\downarrow) \mathbf{m}, \quad (7)$$

where $\mu_F^{\uparrow(\downarrow)} = \int_{\epsilon_F} d\epsilon f^{\uparrow(\downarrow)}$ and $\sigma_F^{\uparrow(\downarrow)}$ are the electrochemical potential and the conductivity for the spin-up (spin-down) electrons, respectively. The spin polarization of the conductivity is defined as $\beta = (\sigma_F^\uparrow - \sigma_F^\downarrow) / (\sigma_F^\uparrow + \sigma_F^\downarrow)$.

The transverse spin accumulation in the ferromagnetic layer obeys¹⁸

$$\frac{\partial^2}{\partial x^2} \mu_F^T = \frac{1}{\lambda_J^2} \mu_F^T \times \mathbf{m} + \frac{1}{\lambda_{\text{sd}(F_T)}^2} \mu_F^T, \quad (8)$$

where $\lambda_J = \sqrt{(D_F^\uparrow + D_F^\downarrow) \hbar / (2J)}$ and $\lambda_{\text{sd}(F_T)}$ is the transverse spin-diffusion length. J is the strength of the exchange field¹⁹ and $D_F^{\uparrow(\downarrow)}$ is the diffusion constant of spin-up (spin-down) electrons. The spin polarization of the diffusion constant is defined as $\beta' = (D_F^\uparrow - D_F^\downarrow) / (D_F^\uparrow + D_F^\downarrow)$. The transverse spin accumulation is expressed as a linear combination of $\exp(\pm x/l_+)$ and $\exp(\pm x/l_-)$, where $1/l_\pm = \sqrt{(1/\lambda_{\text{sd}(F_T)}^2) \mp (i/\lambda_J^2)}$. The penetration depth of the transverse spin current λ_t is defined as $1/\lambda_t = \text{Re}[1/l_+]$.²⁰ The transverse spin current in the ferromagnetic layer is expressed as

$$\mathbf{m} \times (\mathbf{I}_s^F \times \mathbf{m}) = -\frac{\partial}{\partial x} \frac{\hbar S \sigma_F^{\uparrow\downarrow}}{2e^2} \mu_F^T, \quad (9)$$

where $\sigma_F^{\uparrow\downarrow} = [\sigma_F^\uparrow / (1 + \beta') + \sigma_F^\downarrow / (1 - \beta')] / 2$.^{18,20}

The total spin currents across the N_3/F_1 and F_1/N_4 interfaces, i.e., $\mathbf{I}_s^{(1)} = \mathbf{I}_s^{\text{pump}} + \mathbf{I}_s^{F_1/N_3}$ and $\mathbf{I}_s^{(2)} = \mathbf{I}_s^{\text{pump}} + \mathbf{I}_s^{F_1/N_4}$, exert the torque $\boldsymbol{\tau} = \mathbf{m}_1 \times [(\mathbf{I}_s^{(1)} + \mathbf{I}_s^{(2)}) \times \mathbf{m}_1]$ on the magnetization \mathbf{m}_1 . In order to obtain the spin current $\mathbf{I}_s^{(1,2)}$, we solve the diffusion equations of spin accumulations in each layer. The boundary conditions are as follows. We assume that the

thickness of the N_1 and N_7 layer, L_1 and L_7 , are sufficiently thick enough compared to their spin-diffusion length, and that the spin current is zero at the outer boundary of the N_1 and N_7 layers. We also assume that the spin current is continuous at all F_k/N_i and N_i/N_j interfaces and that the electric current is constant through the entire structure. The spin current $\mathbf{I}_s^{(1,2)}$ is obtained as a function of the electric current I and the pumped spin current $\mathbf{I}_s^{\text{pump}}$.

The torque $\boldsymbol{\tau}$ modifies the Landau-Lifshitz-Gilbert (LLG) equation of the magnetization \mathbf{m}_1 . The LLG equation conserves the magnitude of the magnetization, and thus the vectors $\dot{\mathbf{m}}_1$ and $\mathbf{m}_1 \times \dot{\mathbf{m}}_1$ are perpendicular to the magnetization \mathbf{m}_1 . Since the torque $\boldsymbol{\tau}$ is perpendicular to \mathbf{m}_1 , the torque can be decomposed into the directions of $\dot{\mathbf{m}}_1$ and $\mathbf{m}_1 \times \dot{\mathbf{m}}_1$. The LLG equation of \mathbf{m}_1 is expressed as^{20,23,32}

$$\begin{aligned} \frac{d\mathbf{m}_1}{dt} &= -\gamma \mathbf{m}_1 \times \mathbf{B}_{\text{eff}} + \frac{\gamma}{MSd_1} \boldsymbol{\tau} + \alpha_0 \mathbf{m}_1 \times \frac{d\mathbf{m}_1}{dt} \\ &= -\gamma_{\text{eff}} \mathbf{m}_1 \times \mathbf{B}_{\text{eff}} + \frac{\gamma_{\text{eff}}}{\gamma} (\alpha_0 + \alpha') \mathbf{m}_1 \times \frac{d\mathbf{m}_1}{dt}, \quad (10) \end{aligned}$$

where \mathbf{B}_{eff} is the effective magnetic field. $\alpha' = \alpha_c + \alpha_{\text{pump}}$ represents the enhancement of the Gilbert damping constant. The enhancement α_c is proportional to the electric current I and independent of the pumped spin current $\mathbf{I}_s^{\text{pump}}$. The enhancement α_{pump} represents the contribution from the pumped spin current and is independent of the electric current. It should be noted that the enhancement α_{pump} differs from the result of the conventional spin-pumping theory²⁴ because α_{pump} is a function of λ_t . The enhancement of the gyromagnetic ratio $\gamma_{\text{eff}}/\gamma$ is also a function of the electric current and the pumped spin current.

Let us move to the analysis of experimental results of Ref. 12. In general, the dynamics of the magnetization \mathbf{m}_1 determined by Eq. (10) is very complicated; thus, we cannot obtain the analytical expression of the critical current of STT-driven magnetization dynamics of the magnetization \mathbf{m}_1 . However, in the experiment of Ref. 12, the system, and therefore the dynamics of \mathbf{m}_1 , have axial symmetry along the direction normal to the film plane because the high magnetic field (about 7 T) is applied along this direction. Then we assume that the magnetization of the F_1 layer \mathbf{m}_1 precesses around the magnetization of the F_2 layer \mathbf{m}_2 with the relative angle θ and the angular frequency ω . The critical current of STT-driven magnetization dynamics is defined by the current that satisfies the condition, $\alpha_0 + \alpha_c + \alpha_{\text{pump}} = 0$. The critical current I_c is expressed as

$$I_c = \frac{2eMSd_1}{\hbar \gamma \tilde{\eta}} (\alpha_0 + \alpha_{\text{pump}}) \omega, \quad (11)$$

where $\tilde{\eta}$ is the effective transverse spin-polarization coefficient that is determined by the diffusion equations of the spin accumulations, and thus the coefficient $\tilde{\eta}$ is the function of $d_1/\lambda_{\text{sd}(F_1)}$ and d_1/l_{\pm} .

The parameters we used are as follows. The system consists of nine layers shown in Fig. 1, where F_1 and F_2 are Co, N_1 , N_3 , N_4 , N_5 , and N_7 are Cu, and N_2 and N_6 are Pt. The

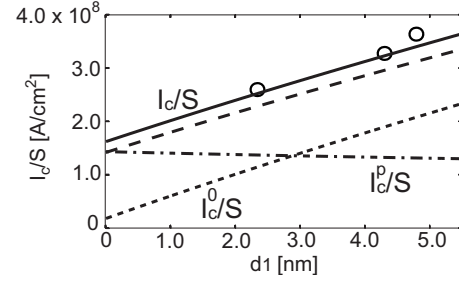


FIG. 2. The critical current density vs the thickness of the free (F_1) layer. The circles are the experimental result of Chen *et al.* (Ref. 12) for 70×140 nm² junctions. The solid line corresponds to I_c/S [see Eq. (11)]. The dotted and dashed-dotted lines correspond to I_c^0/S and I_c^p/S , respectively. The dashed line corresponds to I_c/S in the limit of $\lambda_t \rightarrow 0$.

thicknesses of the N_3 , N_4 , and N_5 layers are 10 nm, the thicknesses of the N_2 and N_6 layers are 3 nm, and the thickness of the F_2 layer is 12 nm.¹² The thickness of the N_1 and N_7 layers are taken to be 10 μm , which is sufficiently longer than the spin-diffusion length. The resistivity $(2\sigma_N)^{-1}$ of Cu and Pt are 14 and 42 Ω nm, respectively.³³ The spin-diffusion length λ_N of Cu and Pt are 1000 and 14 nm, respectively.³³ The conductance at the Cu/Pt interface $g_{\text{Cu/Pt}}/S$ is 35 nm⁻².³³ The magnetization M , the intrinsic Gilbert damping constant α_0 , and the gyromagnetic ratio γ of Co are 0.14 T, 0.008, and 1.89×10^{11} Hz/T, respectively.^{12,34} For simplicity, we assume that $p = \beta = \beta' = 0.46$ for Co.³³ The resistivity $(\sigma_F^{\uparrow} + \sigma_F^{\downarrow})^{-1}$ and the longitudinal spin-diffusion length $\lambda_{\text{sd}(F_1)}$ of the Co are 60 Ω nm and 40 nm, respectively.³³ The transverse spin-diffusion length is $\lambda_{\text{sd}(F_1)} = \lambda_{\text{sd}(F_1)} / \sqrt{1 - \beta^2}$.¹⁸ λ_J is taken to be 3.0 nm,¹⁹ i.e., $\lambda_t = 4.2$ nm. The conductances at the Co/Cu interface, g/S , $g_r^{\uparrow\downarrow}/S$, and $g_i^{\uparrow\downarrow}/S$, are 50, 27, and 0.4 nm⁻², respectively.^{23-26,35} The angular frequency is $\omega = \gamma(B_{\text{appl}} + 4\pi M)$, where the strength of the applied magnetic field B_{appl} is 7 T.¹² The relative angle of the two magnetizations θ is assumed to be 0.99π .¹² Although there are many material parameters in our calculation, these values except $t_{r,i}^{\uparrow\downarrow}$ are determined by the experiments and *ab initio* calculations. The value of $t_{r,i}^{\uparrow\downarrow}/S$ is determined by fitting, and taken to be 6.0 nm⁻². According to Ref. 12, the experimental values are the low-temperature values.

The obtained critical current density is plotted by a solid line against the thickness of the free layer d_1 in Fig. 2. The experimental results of Ref. 12 are shown by open circles. One can see that our results agree well with the experimental results. The critical current density decreases as the thickness of the free layer decreases, and remains finite even in the zero-thickness limit of the free layer. In order to see the main mechanism that determines the remaining value of the critical current density, we decompose I_c of Eq. (11) into two parts as $I_c = I_c^0 + I_c^p$, where I_c^0 is the component proportional to α_0 and I_c^p is the component proportional to α_{pump} . In Fig. 2, the components I_c^0/S and I_c^p/S are plotted by dotted and dot-dashed lines, respectively. As shown in Fig. 2 the remaining value of the critical current in the limit of $d_1 \rightarrow 0$ is determined mainly by the spin pumping. Although I_c^0/S is also

finite in the limit of $d_1 \rightarrow 0$ because of the finite penetration depth of the transverse spin current λ_t in the F_1 layer, the remaining value is small compared to I_c^p/S . The dashed line in Fig. 2 is the calculated critical current I_c/S in the limit of $\lambda_t \rightarrow 0$. According to Fig. 2 we conclude that the effect of the finite penetration depth λ_t is less important in describing the results of Ref. 12.

The reason why both I_c^0 and I_c^p remain finite in the limit of $d_1 \rightarrow 0$ is understood as follows. Slonczewski¹ assumed that the transverse spin current injected into the free layer is absorbed at the interface, and thus, STT is independent of the thickness of the free layer. The critical current is determined by the competition between STT and the magnetic (Gilbert) damping of the free layer. The spin relaxation due to the Gilbert damping is proportional to the thickness of the free layer d_1 , and thus, the critical current given by Eq. (1) is proportional to d_1 and vanishes in the limit of $d_1 \rightarrow 0$. If the penetration depth of the transverse spin current λ_t is finite, the transverse spin current is not fully absorbed in the free layer in the case of $d_1 \ll \lambda_t$. Then the strength of STT is decreased compared to the prediction of Slonczewski,¹ and thus, the critical current is increased. Spin pumping enhances the Gilbert damping, and the spin relaxation due to spin pumping is independent of the thickness of the free layer. Thus, I_c^p remains finite in the limit of $d_1 \rightarrow 0$.

The dependences of the remaining value, about 1.6×10^8 A/cm², on the parameters given above are as follows. If the resistivity and the longitudinal spin-diffusion length of Co are taken to be 210 Ω nm and 38 nm, respectively, which are the room-temperature values,³³ the remaining value is estimated to be 1.5×10^8 A/cm². The reduction of the longitudinal spin-diffusion length decreases the penetration depth λ_r , and thus, the remaining value is reduced. The values of conductances, g and $g_{r,i}^{\uparrow\downarrow}$, include the effect of the Sharvin conductance.²⁶ If g/S , $g_r^{\uparrow\downarrow}/S$, and $g_i^{\uparrow\downarrow}/S$ are taken to be 19.3, 14.6, and -1.1 nm⁻², respectively, which are the bare values estimated by *ab initio* calculation,²⁶ the remaining value is estimated to be 1.0×10^8 A/cm². The reduction in the mixing conductance decreases the effect of spin pumping,²³ and thus, the remaining value is reduced. If the transmission mixing conductance $t_{r,i}^{\uparrow\downarrow}/S$ is taken to be 3.0(12.0) nm⁻², which is half (twice) compared to the value used in Fig. 2, the remaining value is estimated to be $1.5(1.8) \times 10^8$ A/cm². The reduction (enhancement) of the transmission mixing conductance decreases (increases) the effect of the transverse spin accumulation, or equivalently the penetration depth, on the spin current given by Eq. (4), and thus, the remaining value is reduced (enhanced). We conclude that although there are many material parameters in our calculation the parameter dependence of the remaining value is small, and our calculation gives the correct order of the critical current.

The above results imply that we can increase or decrease the critical current by controlling the spin pumping. Spin pumping is the phenomenon by which the precessing magnetization of the free layer pumps spin current into the other layers. The other layers act as an additional spin sink and the magnetic damping of the free layer is enhanced by spin pumping. The ability of the spin sink is determined by the spin-diffusion length since the spin-diffusion length is in-

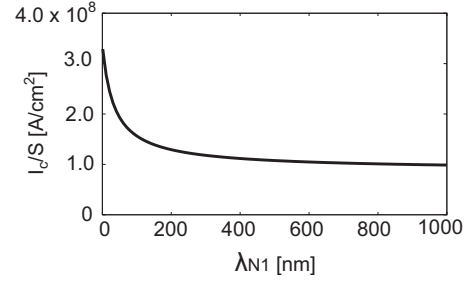


FIG. 3. The dependence of the critical current in the zero-thickness limit of the free layer in the $N_1/F_1/N_4/F_2/N_7$ five-layer system on the spin-diffusion length of the N_1 layer, λ_{N_1} .

versely proportional to the square root of the spin scattering rate. Materials with short (long) spin-diffusion length act as a good (bad) spin sink. One may expect that, if the nonmagnetic layer adjacent to the free layer is made of material with a long spin-diffusion length, the Gilbert damping constant and, therefore, the critical current is suppressed. In the limit of infinite spin-diffusion length, $\lambda_N \rightarrow \infty$, there is no spin-flip scattering in the nonmagnetic layer and the spin pumping into the nonmagnetic layer is forbidden. On the other hand, if the nonmagnetic layer adjacent to the free layer is made of a material with a short spin-diffusion length, the Gilbert damping constant and the critical current are enhanced. In the limit of $\lambda_N \rightarrow 0$, the pumped spin current is absorbed at the interface and enhancement of the critical current due to spin current is maximized.

In order to verify the above statement, we analyzed the critical current of the five-layer system, $N_1/F_1/N_4/F_2/N_7$ (see Fig. 1), where all parameters except the spin-diffusion length of the N_1 layer, λ_{N_1} , are the same as those used in the analysis of Chen's experiment. In Fig. 3, we plot the critical current in the zero-thickness limit of the free layer as a function of the spin-diffusion length of the N_1 layer λ_{N_1} . One can see that the critical current is a decreasing function of λ_{N_1} . The critical current remains finite in the limit of $\lambda_N \rightarrow \infty$ because of the spin pumping into the N_4 layer and the finite penetration depth of the transverse spin current. The result shown in Fig. 3 shows that we can control the critical current by varying the spin-diffusion length of the nonmagnetic electrode adjacent to the free layer.

We cannot apply the present formula directly to a magnetic tunnel junction (MTJ) because spin accumulation is not well defined in an insulator (I). Although the spin pumping across the insulating barrier is beyond the scope of this paper, the spin pumping into the metallic electrode should give the finite remaining value of the critical current. Recently spin pumping in a MTJ was studied by Moriyama *et al.*³⁶ They studied a ferromagnetic resonance in Al/AIO/Ni₈₀Fe₂₀/Cu MTJ and found the generation of the voltage on the order of a few microvolts, which is qualitatively explained by the theory of spin pumping in a metallic structure³⁷ but requires an unreasonably large value of mixing conductance. The results of Moriyama *et al.*³⁶ suggest that a different nonequilibrium phenomenon exists in MTJ, e.g., charge pumping or the development of the longitudinal spin accumulation in a ferromagnetic layer.³⁸

In conclusion, we studied the critical current of spin-transfer-torque-driven magnetization dynamics by taking into account both the finite penetration depth of the transverse spin current in the ferromagnetic layer and spin pumping. We extend the spin-pumping theory with the finite penetration depth to include the electric current and successfully reproduced the experimental results of Ref. 12. We showed that the critical current remains finite in the zero-thickness

limit of the free layer and the remaining value is determined mainly by spin pumping. We also showed that we can control the remaining value of the critical current by varying the spin-diffusion length of the nonmagnetic electrode adjacent to the free layer.

The authors would like to thank W. Chen, A. D. Kent, and their co-workers for providing their experimental results. This work was supported by JSPS and NEDO.

*Corresponding author; h-imamura@aist.go.jp

- ¹J. C. Slonczewski, *J. Magn. Magn. Mater.* **159**, L1 (1996).
- ²L. Berger, *Phys. Rev. B* **54**, 9353 (1996).
- ³J. A. Katine, F. J. Albert, R. A. Buhrman, E. B. Myers, and D. C. Ralph, *Phys. Rev. Lett.* **84**, 3149 (2000).
- ⁴K. Carva, I. Turek, J. Kudrnovský, and O. Bengone, *Phys. Rev. B* **73**, 144421 (2006).
- ⁵P. M. Haney, D. Waldron, R. A. Duine, A. S. Núñez, H. Guo, and A. H. MacDonald, *Phys. Rev. B* **76**, 024404 (2007).
- ⁶C. Heiliger and M. D. Stiles, *Phys. Rev. Lett.* **100**, 186805 (2008).
- ⁷H. Kubota *et al.*, *Nat. Phys.* **4**, 37 (2008).
- ⁸J. C. Sankey, Y.-T. Cui, J. Z. Sun, J. C. Slonczewski, R. A. Buhrman, and D. C. Ralph, *Nat. Phys.* **4**, 67 (2008).
- ⁹S. I. Kiselev, J. C. Sankey, I. N. Krivorotov, N. C. Emley, R. J. Schoelkopf, R. A. Buhrman, and D. C. Ralph, *Nature (London)* **425**, 380 (2003).
- ¹⁰T. Seki, S. Mitani, K. Yakushiji, and K. Takanashi, *Appl. Phys. Lett.* **89**, 172504 (2006).
- ¹¹A. Deac, K. J. Lee, Y. Liu, O. Redon, M. Li, P. Wang, J. P. Nozières, and B. Dieny, *Phys. Rev. B* **73**, 064414 (2006).
- ¹²W. Chen, M. J. Rooks, N. Ruiz, J. Z. Sun, and A. D. Kent, *Phys. Rev. B* **74**, 144408 (2006).
- ¹³A. Tanaka, Y. Shimizu, Y. Seyama, K. Nagasaka, R. Kondo, H. Oshima, S. Eguchi, and H. Kanai, *IEEE Trans. Magn.* **38**, 84 (2002).
- ¹⁴M. Takagishi, K. Koi, M. Yoshikawa, T. Funayama, H. Iwasaki, and M. Sahashi, *IEEE Trans. Magn.* **38**, 2277 (2002).
- ¹⁵J.-G. Zhu and X. Zhu, *IEEE Trans. Magn.* **40**, 182 (2004).
- ¹⁶J. Grollier, V. Cros, H. Jaffrés, A. Hamzic, J. M. George, G. Faini, J. B. Youssef, H. LeGall, and A. Fert, *Phys. Rev. B* **67**, 174402 (2003).
- ¹⁷H. Morise and S. Nakamura, *Phys. Rev. B* **71**, 014439 (2005).
- ¹⁸S. Zhang, P. M. Levy, and A. Fert, *Phys. Rev. Lett.* **88**, 236601 (2002).
- ¹⁹J. Zhang, P. M. Levy, S. Zhang, and V. Antropov, *Phys. Rev. Lett.* **93**, 256602 (2004).
- ²⁰T. Taniguchi, S. Yakata, H. Imamura, and Y. Ando, *Appl. Phys. Express* **1**, 031302 (2008).
- ²¹S. Mizukami, Y. Ando, and T. Miyazaki, *J. Magn. Magn. Mater.* **239**, 42 (2002).
- ²²S. Mizukami, Y. Ando, and T. Miyazaki, *Phys. Rev. B* **66**, 104413 (2002).
- ²³Y. Tserkovnyak, A. Brataas, and G. E. W. Bauer, *Phys. Rev. B* **66**, 224403 (2002).
- ²⁴Y. Tserkovnyak, A. Brataas, and G. E. W. Bauer, *Phys. Rev. B* **67**, 140404(R) (2003).
- ²⁵A. Brataas, Y. V. Nazarov, and G. E. W. Bauer, *Eur. Phys. J. B* **22**, 99 (2001).
- ²⁶M. Zwierzycki, Y. Tserkovnyak, P. J. Kelly, A. Brataas, and G. E. W. Bauer, *Phys. Rev. B* **71**, 064420 (2005).
- ²⁷G. E. W. Bauer, Y. Tserkovnyak, D. Huertas-Hernando, and A. Brataas, *Phys. Rev. B* **67**, 094421 (2003).
- ²⁸J. C. Slonczewski, *Phys. Rev. Lett.* **96**, 019707 (2006).
- ²⁹S. Urazhdin, R. Loloee, and W. P. Pratt, *Phys. Rev. B* **71**, 100401(R) (2005).
- ³⁰J. Guo and Mansoor Bin Abdul Jalil, *Phys. Rev. B* **71**, 224408 (2005).
- ³¹T. Valet and A. Fert, *Phys. Rev. B* **48**, 7099 (1993).
- ³²T. Taniguchi and H. Imamura, *Phys. Rev. B* **76**, 092402 (2007).
- ³³J. Bass and W. P. Pratt, Jr., *J. Phys.: Condens. Matter* **19**, 183201 (2007).
- ³⁴J.-M. L. Beaujour, W. Chen, A. D. Kent, and J. Z. Sun, *J. Appl. Phys.* **99**, 08N503 (2006).
- ³⁵K. Xia, P. J. Kelly, G. E. W. Bauer, A. Brataas, and I. Turek, *Phys. Rev. B* **65**, 220401(R) (2002).
- ³⁶T. Moriyama, R. Cao, X. Fan, G. Xuan, B. K. Nikolić, Y. Tserkovnyak, J. Kolodzey, and J. Q. Xiao, *Phys. Rev. Lett.* **100**, 067602 (2008).
- ³⁷X. Wang, G. E. W. Bauer, B. J. van Wees, A. Brataas, and Y. Tserkovnyak, *Phys. Rev. Lett.* **97**, 216602 (2006).
- ³⁸Y. Tserkovnyak, T. Moriyama, and J. Q. Xiao, *Phys. Rev. B* **78**, 020401(R) (2008).